



Cite this: *Soft Matter*, 2023, **19**, 8779

Received 22nd August 2023,  
Accepted 14th October 2023

DOI: 10.1039/d3sm01105d

[rsc.li/soft-matter-journal](http://rsc.li/soft-matter-journal)

## A simple method to alter the binding specificity of DNA-coated colloids that crystallize†

Pepijn G. Moerman, <sup>ab</sup> Huang Fang, <sup>cd</sup> Thomas E. Videbæk, <sup>c</sup> W. Benjamin Rogers \*<sup>c</sup> and Rebecca Schulman \*<sup>aef</sup>

DNA-coated colloids can crystallize into a multitude of lattices, ranging from face-centered cubic to diamond, opening avenues to producing structures with useful photonic properties. The potential design space of DNA-coated colloids is large, but its exploration is hampered by a reliance on chemically modified DNA that is slow and expensive to commercially synthesize. Here we introduce a method to controllably tailor the sequences of DNA-coated particles by covalently appending new sequence domains onto the DNA grafted to colloidal particles. The tailored particles crystallize as readily and at the same temperature as those produced *via* direct chemical synthesis, making them suitable for self-assembly. Moreover, we show that particles coated with a single sequence can be converted into a variety of building blocks with differing specificities by appending different DNA sequences to them. This method will make it practical to identify optimal and complex particle sequence designs and paves the way to programming the assembly kinetics of DNA-coated colloids.

## 1 Introduction

Thanks to the specificity of DNA hybridization, orthogonal interactions can be prescribed between microscopic objects by coating the objects with orthogonal, complementary pairs of single-stranded DNA;<sup>1–3</sup> building blocks with complementary sequences have short-ranged attractive interactions resulting from the hybridization of the DNA on their surfaces.<sup>4</sup> This use of DNA is an established strategy for producing building blocks that can assemble into a wide variety of microscopic structures, including stick figures,<sup>5</sup> crystal lattices,<sup>6–9</sup> flexible bead-chains,<sup>10,11</sup> chiral clusters,<sup>12</sup> and even cell aggregates.<sup>13</sup> Because DNA-coated microparticles (Fig. 1a) have sizes comparable to the wavelength of visible light, they are particularly promising building blocks for the self-assembly of photonic bandgap materials,<sup>14–17</sup> with applications in optical wave guides, lasers, and various light-harvesting technologies.

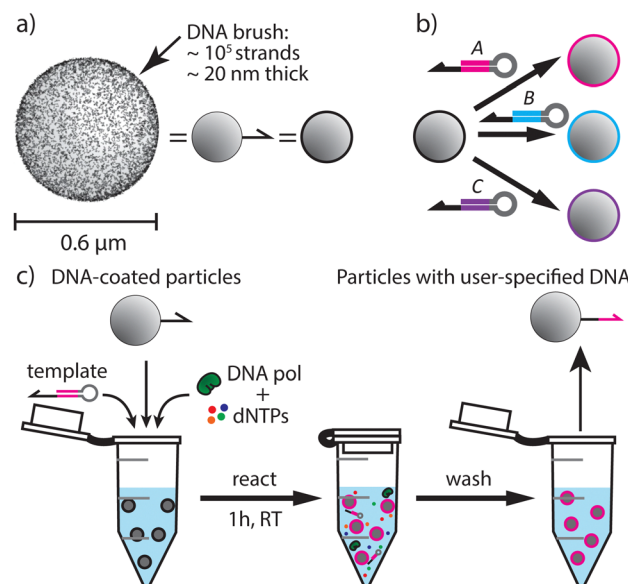


**Fig. 1** (a) Schematic of DNA-coated colloids. Cartoon of DNA brush on colloid is copied from ref. 1. (b) The primer exchange reaction enables the production of a range of DNA-coated colloids with distinct binding specificities from a single particle feed stock. (c) Overview of the primer exchange reaction (PER) that extends the DNA on DNA-coated particles. DNA polymerase, a deoxynucleotide triphosphate (dNTP) mixture, and a DNA sequence template are mixed in an Eppendorf tube and left at room temperature. Then the particles are separated from the reaction mixture by centrifugation, at which point they are ready to be used in self-assembly experiments.

<sup>a</sup> Department of Chemical and Biomolecular Engineering, Johns Hopkins University, Baltimore, MD 21218, USA. E-mail: rschulm3@jhu.edu

<sup>b</sup> Department of Chemical Engineering and Chemistry, Eindhoven University of Technology, 5612 AE Eindhoven, The Netherlands

<sup>c</sup> Martin A. Fisher School of Physics, Brandeis University, Waltham, MA 02453, USA. E-mail: wrogers@brandeis.edu

<sup>d</sup> State Key Laboratory of Surface Physics and Department of Physics, Fudan University, Shanghai, China

<sup>e</sup> Department of Chemistry, Johns Hopkins University, Baltimore, MD 21218, USA

<sup>f</sup> Department of Computer Science, Johns Hopkins University, Baltimore, MD 21218, USA

† Electronic supplementary information (ESI) available. See DOI: <https://doi.org/10.1039/d3sm01105d>



DNA-coated microparticles are also useful as model systems for self-assembly of both equilibrium<sup>18</sup> and energy-dependent systems.<sup>19,20</sup>

DNA can be grafted onto colloidal particles in various ways, but not all methods produce particles that are compatible with equilibrium assembly of colloidal crystals.<sup>21</sup> When biotin-streptavidin chemistry is used to attach single-stranded DNA to particles, the particles tend to hit-and-stick and become kinetically trapped in fractal-like aggregates, even at temperatures at which the DNA-mediated interactions are reversible.<sup>22,23</sup> Strategies to attach DNA to particles based on strain-promoted click chemistry<sup>24–26</sup> produce DNA-coated colloids that crystallize,<sup>17,27,28</sup> but come at the cost of requiring DBCO(dibenzocyclooctyne)-modified DNA which is expensive and time-consuming to commercially synthesize<sup>29</sup> (the DBCO-modification is attached to the 5' end of the DNA and facilitates a click reaction to azide-functionalized particles). The methods have in common that, once the DNA is grafted, the particles' sequences and thus their binding specificities for other particles are fixed. Having a way to change DNA-coatings on self-assembly building blocks after their synthesis would enable conversion of a single feedstock of DNA-coated colloids into a range of building blocks with varying sequences, facilitating fast sequence optimization. It would make possible the recycling of expensive DNA-coated building blocks, and—if the conversion kinetics can be controlled—pave the way to programming the time-evolution of the inter-particle interactions.

Here we introduce a controlled yet permanent way to change the binding specificity of DNA-coated particles by appending user-prescribed sequences onto particle-grafted DNA (Fig. 1b). We use the primer exchange reaction (PER), introduced by Kishi *et al.* in 2019,<sup>30</sup> to append a user-specified domain to the end of an input DNA sequence coating the particle. We show that this reaction can completely update the particles' DNA sequence within 1 hour (Fig. 1c). Particles synthesized using PER—from now on referred to as PER-edited particles—assemble as readily and have the same melting temperature as particles produced directly *via* click chemistry—from now on referred to as reference particles. We also show that a single type of DNA-coated particle can be updated into a variety of particles with different DNA sequences and binding specificities (Fig. 1b).

## 2 Results and discussion

### 2.1 Reaction rate

We first ask whether the primer exchange reaction can be used to append new sequence domains onto DNA-coated colloids. The primer exchange reaction (schematically depicted in Fig. 2) involves the reversible hybridization of a single-stranded input,  $I$ , to the input-binding domain,  $I'$ , of a catalytic hairpin. When  $I$  and  $I'$  are bound, DNA polymerase produces the complement to the hairpin's template sequence,  $A'$ , appending the  $A$  domain onto the input strand, resulting in a longer single-stranded output,  $IA$  (Fig. 2a). The catalytic hairpin strand, which is only weakly bound to the output strand, is eventually released and can bind another input strand.

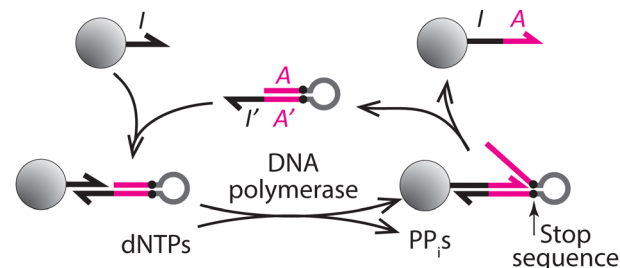


Fig. 2 Schematic of the primer exchange reaction. dNTPs are DNA nucleotides and PP<sub>i</sub>s are inorganic pyrophosphates. The input sequence,  $I$ , is 9 nucleotides, and the output domain,  $A$ , is 11 nucleotides. Sequences are in the ESI† (Section S1). To stop the DNA polymerase from copying more DNA after it has copied the output domain, an artificial stop sequence is incorporated in the template. This stop sequence consists of two nucleotides of which the complement cannot be incorporated because the corresponding dNTP is not present in the reaction mixture. For example, in a solution that lacks dGTP, the incorporation of a G stops the polymerase. More details on designing stop sequences are provided in Section S2 of the ESI†.

The particles whose DNA we set out to “edit” using PER are 600 nm and 1000 nm-diameter polystyrene colloids with single-stranded DNA grafted onto their surface *via* the click chemistry method developed by Oh *et al.*<sup>25</sup> (see Experimental Section). The grafted sequence consists of a 40-nucleotide poly-T spacer followed by a 9-nucleotide input domain,  $I$ . We measured a grafting density of  $3.6 \pm 0.2 \times 10^4$  strands per  $\mu\text{m}^2$  on these particles (Fig. S4, ESI†).

To test whether PER could append a new domain onto the DNA on the 600 nm particles, we mixed the particles at 0.1% (v/v) with 1–100 nM hairpin strand, 100  $\mu\text{M}$  of each nucleotide triphosphate, and 0.13 U  $\mu\text{L}^{-1}$  DNA polymerase, and let the reaction proceed at room temperature for varied reaction times (typically 1 hour). After the reaction, we washed the particles by centrifugation and resuspension. See the Experimental Section for details on the synthesis and ESI† Section S1 for the DNA sequences.

To quantify the PER conversion of DNA on the DNA-coated colloids, we added fluorescently labeled strands to the particles after the reaction and measured the fluorescent signal of ten thousand individual particles using flow cytometry (detailed methods in Experimental Section). The fluorescently labeled DNA strands had sequence  $A'$  and thus could only bind to PER-edited particles. Therefore, the fluorescent signal of each particle is a measure of the fraction of its DNA that has been updated (Fig. 3a). We determined the percent yield of the reaction by comparing the fluorescence intensity of PER-edited particles to that of reference particles to which the sequence  $IA$  (the target sequence of the PER reaction) was attached directly *via* click chemistry (gray shaded curve in Fig. 3b). When 10 nM hairpin was used in the PER reaction, conversion of the DNA on the particles was complete after 8 hours (Fig. 3b). The width of the observed fluorescence histogram is a measure for the spread in the particle fluorescence intensities within the measured particle population, but for narrow distributions—as is the case in our experiments—it is limited to the instruments precision.



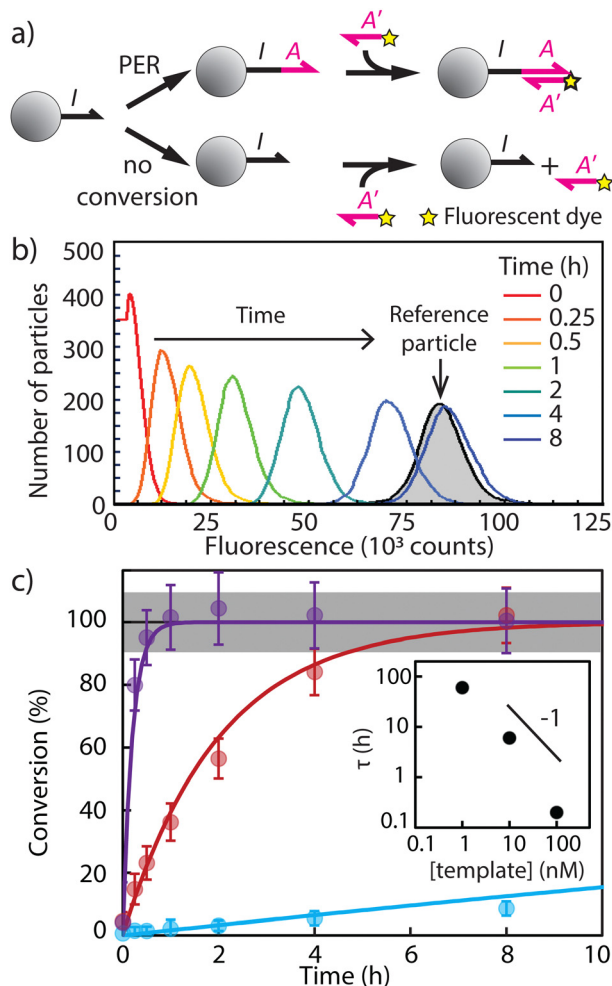


**Fig. 3** (a) Schematic of the labeling reaction used to quantify the DNA conversion on particles. The fluorescently labeled strand with sequence *A'* is complementary to the DNA on PER-edited particles, but not to the input sequence so that the amount of fluorescence indicates the degree of conversion. (b) Histograms showing the distribution of the single-particle fluorescence of DNA-coated particles after increasing reaction times, as measured using flow cytometry. The average fluorescence is a measure of conversion. The gray shaded region indicates the fluorescence of reference particles to which the sequence *A'* was attached through click chemistry. Details of flow cytometry experiments are provided in the ESI† (Experimental Section S4.4). Each histogram represents ten thousand particles. The template concentration was 10 nM. (c) PER conversion as function of time for 1 nM (blue), 10 nM (red), 100 nM (purple) template concentrations. Higher template concentrations lead to faster conversion. Error bars represent the standard deviations of the fluorescence distributions. The particles are 600 nm in diameter. The inset shows the typical reaction time,  $\tau$ , as a function of template concentration. The inset shows that the typical reaction time  $\tau$  scales linearly with the inverse template concentration.

Measurements of particle fluorescence after increasing reaction times indicated that the average conversion per particle increases monotonically until complete conversion is reached. Notably, when the conversion is partial, similar fractions of DNA on each particle are converted. In other words, no two subpopulations exist of entirely unconverted and entirely converted particles (Fig. 3b). This observation suggests that by tuning the

reaction time, a controllable fraction of the DNA on DNA-coated colloids can be edited with PER.

To test whether we could tune the conversion rate, we varied the concentration of catalytic hairpin used in the PER reaction. Fig. 3c shows the conversion as a function of the reaction time for hairpin concentrations of 1 nM, 10 nM, and 100 nM. We found that the two highest concentrations reach complete conversion with a rate that increases approximately linearly with hairpin concentration. The time to complete conversion was 1 hour with 100 nM hairpin and 8 hours with 10 nM hairpin (Fig. 3c). With 1 nM hairpin, the reaction did not go to completion within 7 days (Fig. S1, ESI†). Fitting the measured conversion as a function of time to a single exponential yielded estimates of the typical reaction time when 1/e of the reactant was converted (inset Fig. 3c). We measured values that are a factor of 3 larger than predictions based on the rates of the PER reaction in solution (Fig. S1, ESI†).<sup>31</sup> The decreased PER rate when the substrate DNA is grafted onto colloidal particles compared to DNA free in solution is likely due to the steric hindrance of the DNA polymerase in the dense DNA coating.

Fig. 3c shows that the rate with which new DNA domains are appended onto DNA-coated colloids can be varied over three orders of magnitude by simply changing the template concentration. The tunability of this reaction rate provides control over the time-evolution of DNA-mediated interactions that could be used to initiate sequential assembly stages and freeze objects into kinetically trapped structures.

To check whether any unintended side products formed, we also performed PER on particles coated with streptavidin to which biotinylated DNA was attached (Fig. S2, ESI†). The streptavidin-biotin bond can be broken by heat denaturing streptavidin at 95 °C in 50% formamide solution.<sup>32</sup> Using this method, we removed the DNA from the surfaces of the particles after the primer exchange reaction and analyzed the product sequences using gel electrophoresis. From this experiment we learned that only DNA strands with lengths that correspond to the lengths of the reactant and product sequences were present on the particles after the reaction. No significant concentrations of unintended side products were formed (Fig. S2, ESI†).

## 2.2 Melting temperature

Our PER-editing method is intended to produce self-assembly building blocks, so we next asked whether PER-edited particles have similar assembly properties to the reference particles. Typically, when a binary system of colloids coated with complementary single-stranded DNA sequences is combined, the particles form aggregates below a transition temperature, called the melting temperature. Above the melting temperature the colloids are unaggregated and form a stable dispersion.<sup>1</sup> The melting temperature increases with the magnitude of the hybridization free energy of the DNA strands involved in the inter-particle binding and with their grafting density,<sup>34</sup> so if the PER-edited particles and the reference particles have the same grafting density and sequence, as we expect based on the flow cytometry data, their melting temperature should also be the same.

To determine the melting temperature we prepared samples containing either the reference particles or the PER-edited particles, and particles to which DNA containing a 7-nucleotide complementary domain was attached, which we call co-assemblers. We placed these samples on a custom-built heating element (Experimental Section 4.3) on a microscope and found that both samples had aggregated. We then heated the sample slowly to the melting temperature, *i.e.* the temperature at which approximately half the particles were part of aggregates and half were dispersed. Measurements of the fraction of single particles as function of the temperature are shown in the Supplementary Information (Fig. S6, ESI<sup>†</sup>). While observing the behavior of particles during heating with a 60× oil-immersion lens, the thermistor on our heating stage showed that aggregates of PER-edited particles and their co-assemblers melted at 63 °C and aggregates of the reference particles and their co-assemblers at 65 °C (Fig. 4). These measurements indicate that both particles have similar binding free energies. The 60× oil immersion objective changes the thermal load of the sample, so that the actual temperature of the sample may be lower than that reported by the temperature controller. Indeed, with a 40× air objective we found melting temperatures around 52 °C for reference particles and 50 °C for PER-edited particles.

The finding that there is no observable difference in DNA grafting density between PER-edited particles and the reference particles (Fig. 3) suggests that the slightly decreased melting temperature of the PER-edited particles comes from errors in the sequence. These errors could arise due to the inherent error

rate of Bst DNA polymerase or copying of incorrect or incomplete DNA templates. The 2-degree difference in melting temperature could be explained by one mismatched base pair in 10% of the strands.<sup>33</sup>

### 2.3 Crystallization

Below the melting temperature, the structure that corresponds to a global minimum in the free energy landscape for a binary mixture of same-size DNA-coated colloids is a crystal lattice, isostructural to cesium chloride,<sup>27</sup> that maximizes the number of contacts between the complementary particles and the crystal entropy. However, this equilibrium structure is kinetically difficult to reach, and only accessible if the particles can roll on the surface of their neighbours after binding, which requires both a high density and a homogeneous distribution of grafted DNA.<sup>17,21</sup> Both reference particles and input particles for PER are produced in a way that results in a DNA coating that facilitates crystallization, so we asked whether the ability to crystallize is maintained after PER.

We found that both the reference particles and the PER-edited particles crystallized readily when kept near the melting temperature (Fig. 4), indicating that the PER-edited particles are suitable building blocks for equilibrium self-assembly.

The flow cytometry data in Fig. 3 show that a specific fraction of DNA on each particle can be updated by choosing an appropriate template concentration and reaction time. To check if such partially converted particles are also suitable for self-assembly we asked how the melting temperature scales with the percentage of DNA on particles that is converted and

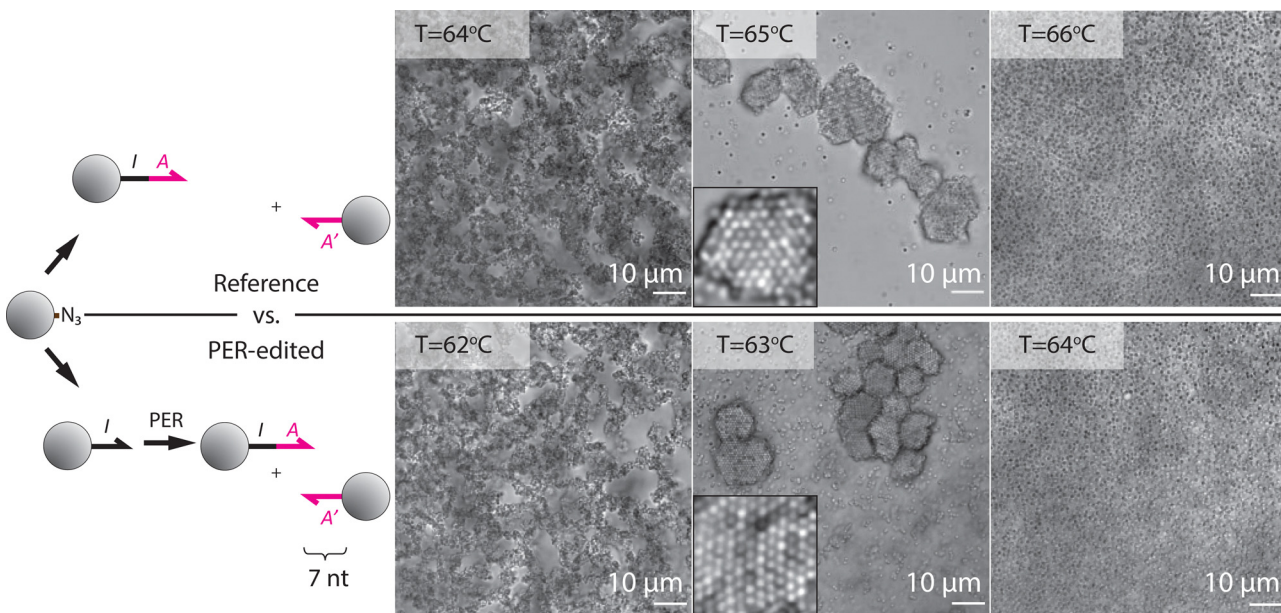


**Fig. 4** The self-assembly of PER-edited particles (bottom row) is compared to that of reference particles (top row). When mixed with particles coated with the complementary DNA sequence, both the reference and PER-edited particles (100% conversion, made with a template concentration of 100 nM and a reaction time of 1 hour) formed random aggregates below the melting temperature, crystallized when held near the melting temperature, and were unassembled above the melting temperature. The insets are high-magnification micrographs of the crystal lattices. The complementary sequence, A', contains 7 consecutive bases complementary with sequence A. All particles are 600 nm in diameter. The images were recorded with an oil-immersion objective which increases thermal contact with the sample so the actual sample temperature is lower than the reported temperature.



what conversion is required for the particles to crystallize. To this end, we prepared PER-edited particles with conversion percentages ranging from 0.1% to 100% by varying the reaction time and template concentration. We mixed these partially converted particles with co-assemblers, similar to the experiment in Fig. 4, and measured the melting temperatures.

As the conversion increases from 0%, the melting temperature also increases until the melting temperature of the reference particles, 52 °C, is reached at approximately 40% conversion. Above 40% conversion the melting temperature plateaued (Fig. 5). The observed increase of the melting temperature is consistent with the increase in melting temperature as a function of grafting density observed in earlier work,<sup>34,35</sup> but the apparent plateau at 40% is surprising. A notable difference with previous studies that could explain this observation is that we only varied the conversion of one of the two binding partners, and kept the grafting density of the other binding partner constant, so that the average grafting density of DNA containing sticky ends involved in the two-particle interaction goes from 50% to 100% as the conversion goes from 0% to 100%. We also found that only particles with conversions over 30% could crystallize with their binding partners. Below that conversion random aggregates formed even at the melting temperature consistent with the notion that crystallization requires a threshold grafting density.<sup>21</sup>

The collapse of the measured melting temperatures as a function of fractional PER conversion for different hairpin concentrations onto a single curve shows that the fraction of DNA that has been updated is the only factor that determines the melting temperature of the PER-edited particles and that the mechanism by which the conversion is reached does not

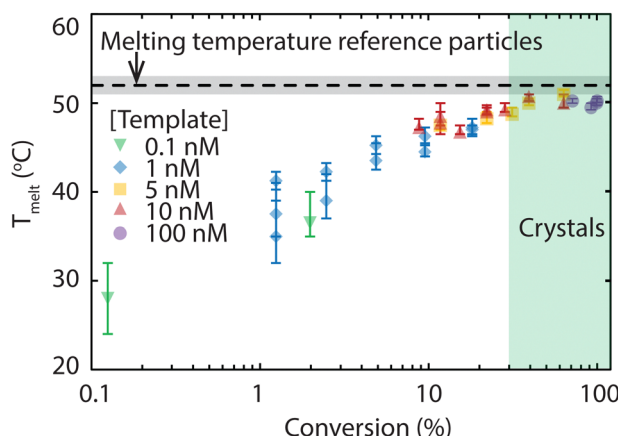


Fig. 5 The melting temperature as a function of approximate conversion. The approximate conversions are calculated using the fits in Fig. 3. The melting temperature increased with conversion and plateaued near the melting temperature of the reference particles (dashed black line). The green area indicates conversions for which we observed that the particles could crystallize. Below 30% conversion, particles did not crystallize even if they were kept near the melting temperature. The melting temperature of unedited particles with the complementary particles is approximately 23 °C, due to partial sequence complementarity between *I* and *I'* (no more than 2 sequential bases). The error bars and gray shaded area indicate the standard deviation of triplicate measurements.

affect the outcome. These findings show that particles with controllable conversion and—by extension—controllable melting temperature can be prepared by tuning the reaction time and catalyst concentration.

The propensity of PER-edited particles to crystallize also depended on the PER conditions. Letting the reaction go for longer than necessary to reach 100% conversion, or using more than 0.13 U  $\mu$ L<sup>-1</sup> Bst DNA polymerase resulted in particles that displayed non-specific aggregation even well above the melting temperature and did not crystallize (Fig. S3, ESI†). The non-specific aggregation could be due to slow primer-independent or template-independent polymerization reactions.<sup>36,37</sup>

#### 2.4. Altering binding specificity

The key advance enabled by our method is that a single feedstock of DNA-coated colloids can be converted into multiple types of self-assembly building blocks with distinct binding specificities. To demonstrate this capability, we show that three different sequences can be appended onto the DNA on one type of “input” particle and that the resultant PER-edited particles have differing binding specificities (Fig. 6).

To this end we converted precursor particles with sequence *I* into assembly building blocks with sequences *IA*, *IB*, and *IC* using 100 nM concentrations of three different templates.

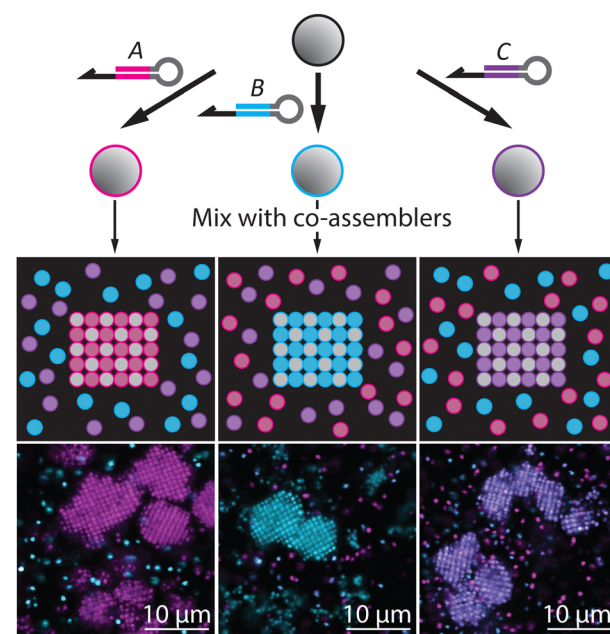
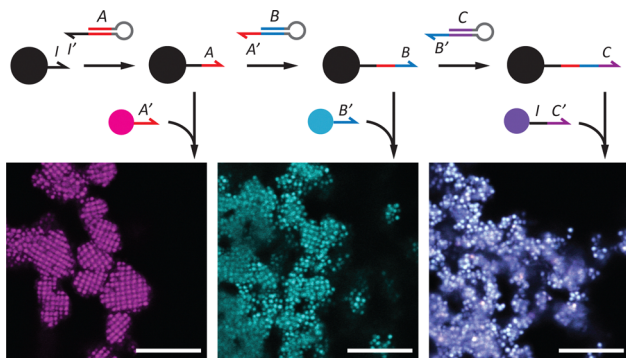


Fig. 6 PER converts a generic DNA-coated particle into three building blocks for self-assembly with differing binding specificities. The input particles (not fluorescently labeled) are converted into three batches of DNA-coated particles with differing sequence: *A*, *B*, and *C*. Each batch is mixed with three types of fluorescently labeled particles: magenta particles are coated with sequence *A'*, cyan particles are coated with *B'*, and purple particles are coated with *C'*. The samples are annealed at the melting temperature and imaged at the melting temperature under a confocal microscope (Left:  $T_m = 59.5$  °C, Middle:  $T_m = 58.4$  °C, Right:  $T_m = 67.5$  °C). Each type of converted particle aggregated only with their respective complementary particle. Scale bars are 10  $\mu$ m.





**Fig. 7** Multi-domain DNA strands can be grown onto colloids via sequential PER reactions. Here the generic input sequence, *I*, is first extended to form output sequence *IA*. Then the *IA* sequence is extended with a *B* domain. Finally the *IAB* sequence is extended with a *C* domain. Particles with the *IA* sequence aggregate with *A'* co-assemblers, particles with the *IAB* sequence aggregate with *B'* co-assemblers, and particles with the *IABC* sequence aggregate with *C'* co-assemblers, indicating that the conversions were successful. The particles with the *IC'* sequence have been PER edited from the *I* precursor particles. Scale bars are 10  $\mu$ m.

We then mixed the three PER-edited particles with a set of three co-assemblers—DNA-coated particles that contain DNA complementary to each of the PER-edited particles: *A'*, *B'*, and *C'*. The co-assembler particles were fluorescently labeled with a magenta dye, a cyan dye, or both the magenta and the cyan dyes (shown as purple), respectively. The PER-edited particles were not fluorescently labeled and are not visible in the images. We annealed a suspension of all four particle types at the melting temperature and imaged the resultant crystals using confocal microscopy. If the single feedstock of DNA-coated particles has successfully been converted into three distinct types of building blocks with differing binding specificities, each of the PER-edited building blocks should bind only to their target co-assembler and leave their off-target co-assembler particles free in solution.

Fig. 6 shows that in each of the three samples, the PER-edited particles indeed co-crystallized only with their intended co-assembler; each of the crystals are either fully magenta, cyan, or purple. Notably, the co-assembler particles for the purple aggregates were also produced from the initial feed stock using the primer exchange reaction, showing that crystals form even if both types of DNA-coated particles in a binary system were produced using PER.

**2.4.1 Sequential sequence altering.** The repeatable modification of a set of colloids is desirable because it would allow recycling of DNA-coated colloids and would introduce a new functionality in self-assembly where the particles specificities could be changed multiple times. Therefore, we tested whether multiple domains could be sequentially attached to a single particle. We tested the sequential attachment of up to three 11-nucleotide domains and found that the binding specificity of the particles successfully changed with each added DNA sequence (Fig. 7). However, particles to which more than one domain was added with PER were not able to crystallize with their complements. The current method thus facilitates

multiple specificity modifications, but not without some loss in functionality. The DNA strands on the particles grow with each subsequent modification, which brings about two problems: 1) the previous specificity is not removed, and 2) the ability to crystallize is lost as the strands grow longer, potentially because the previous sequences contribute to spurious interactions between the colloids. It would be worthwhile to investigate whether DNA domains can be removed with restriction enzymes, so that the particles can be returned to their unmodified form prior to attachment of a new DNA domain.

### 3 Conclusions

We have introduced a method to rapidly and easily alter the binding specificity of DNA-coated colloids by appending new DNA domains onto colloid-grafted DNA strands. We showed that DNA-coated particles with differing binding specificities could be prepared from a single feedstock by appending new domains to the DNA on the colloids and that the particles maintained their ability to crystallize after the DNA extension procedure.

A restriction of the method we presented is that it only allows the addition of sequence domains with a three-letter alphabet (e.g. ACT, but not G), because we used the fourth letter as a stop sequence. For many applications this is only a minor limitation, because the three-letter alphabet is routinely used in DNA nanotechnology as a design rule to prevent the hybridization of DNA strands with spurious targets. Moreover, Kishi *et al.*<sup>30</sup> showed that nonnatural bases can be used as stop sequences in PER, taking away the restriction that a three-letter alphabet be used, but it comes at the cost of templates that are more expensive and time-consuming to make. Future studies are required to investigate whether these strategies can be applied to particle-based PER as well.

Colloid science and self-assembly have a range of open challenges that require access to building blocks with many orthogonal, tunable interactions to be addressed, such as the self-assembly of finite-sized structures of arbitrary shapes and sizes<sup>5,19,38,39</sup> and understanding the nucleation and growth of multi-component crystals.<sup>17,40</sup> DNA-coated particles are convenient building blocks to address these challenges because their DNA-hybridization-mediated interactions enable on the order of 100 orthogonal interactions<sup>41</sup> with tunable strengths. However, the long duration of the synthesis—and importantly the optimization—of DNA-coated colloids has long been a barrier for their use; while the synthesis of DNA-coated particles from DBCO-modified DNA and azide-functionalized particles only takes a day,<sup>25</sup> it takes on the order of 1 month for commercial suppliers to synthesize DBCO-functionalized DNA.<sup>29</sup> This is particularly problematic for sequence optimization. PER-editing particles provides a way to quickly—commercial synthesis of PER templates takes less than one week<sup>29</sup>—produce a wide variety of different DNA-coated colloids from a single feedstock and optimize their designs so applications and experiments requiring many different DNA-coated colloids come within reach.



Our method may also help expand the use of DNA-coated particles beyond crystallization and self-assembly to sub-fields of colloid science such as gelation and rheology.<sup>42–44</sup> This would additionally require addressing the issue of scalable production of DNA-coated colloids.

Our method could potentially be extended beyond particles, to other systems where the grafting of DNA onto a surface is expensive, time-consuming, or difficult, such as cells<sup>13</sup> and antibodies.<sup>45</sup> It could also be extended to change the binding specificity of single probes in DNA micro-arrays.<sup>46</sup>

It is also possible to do PER on chemically modified DNA prior to grafting the DNA to the target surface, but purification of the product is often simpler (centrifugation and resuspension in the case of microparticles) than purification of the DNA (through gel electrophoresis for example).

An alternative method to change the binding specificity of DNA-coated colloids is the addition of linker strands that form bridges between the DNA on two different particles, thereby causing an attractive interaction between the particles.<sup>47</sup> Our PER-based method differs from the addition of linker strands in that it covalently attaches new DNA sequences to the particles, permanently changing their binding specificity and leaving the DNA on the particles single stranded. Additionally, when using linkers to control binding specificity, the binding free energy of the particles depends on the linker concentration, which can be convenient for the fine-tuning of the binding strength, but makes the assembly less robust to variations in linker concentration. This sensitivity causes linker-induced particle aggregates to crystallize only in a narrow range of linker concentrations.<sup>48</sup>

Our work also opens up the possibility of converting precursors into assembly-active building blocks and altering the building blocks' binding properties during the self-assembly process. Such time-dependent interactions are increasingly sought after for their ability to create dynamic, reconfigurable, and adaptive structures, but currently few chemical strategies for achieving time-dependent interaction strengths are available.<sup>49,50</sup> The control over the time-evolution of DNA-mediated interactions that our method provides could be used to initiate sequential assembly stages and freeze objects into kinetically trapped structures by converting the DNA on different particles at varying rates.

## 4 Experimental section

### 4.1 Particle synthesis

We synthesized DNA-grafted colloidal particles (scale: 40  $\mu$ L of a 1 wt% particle suspension) following a modified version of the strain-promoted azide–alkyne cycloaddition method described in ref. 25. In brief, the method is comprised of three steps: (1) Azide groups are attached to the ends of polystyrene-poly(ethylene oxide) (PS-PEO) diblock copolymers; (2) The azide-modified PS-PEO copolymers are physically grafted to the surface of polystyrene colloids; and (3) DBCO-functionalized single-stranded DNA molecules are conjugated to the ends of the grafted

PS-PEO copolymers by strain-promoted click chemistry. The specific protocol we use is described below. For a detailed step-by-step recipe, see the ESI† of ref. 52

We made azide-modified PS-PEO by first functionalizing PS-PEO ( $M_w = 6500$  g mol<sup>−1</sup> PEO and 3800 g mol<sup>−1</sup> PS, Polymer Source Inc.) with a methanesulfonate (Ms) group and then substituting the Ms groups with azide groups. To obtain PS-PEO-Ms, we mixed 100 mg of PS-PEO, 2 mL of dichloromethane (Sigma-Aldrich), and 42  $\mu$ L of triethylamine (Sigma-Aldrich) in a glass vial, and stirred the mixture for 15 minutes on ice. Next we added 23.5  $\mu$ L of methanesulfonyl chloride (471259 Sigma-Aldrich), stirred the solution on ice for 2 hours, removed it from the ice bath and stir at room temperature for 22 hours. After the reaction, we dried the solution overnight in a vacuum dessicator and washed the dried pellet twice with a mixture of 10 mL anhydrous methanol (MeOH) (Sigma-Aldrich) and 243  $\mu$ L of 37% hydrochloric acid (Fischer Scientific), and then twice with a solution of 3 mL of MeOH and 40 mL of diethyl ether (Sigma-Aldrich). In each washing step, we dissolved the pellet and then precipitated the PS-PEO by placing the sample in the freezer for one hour. Then we centrifuged the solution at 4500 rpm at 2 °C for 10 minutes to form a pellet and poured off the supernatant. After washing, we dried the pellet again.

Next, we substituted the Ms groups with azide groups. We mixed 10 mg of sodium azide (S2002-5G, Sigma-Aldrich), 2 mL of dimethylformamide (Sigma-Aldrich), and the dried PS-PEO pellet. We placed the solution in a 65 °C oil bath and stirred at 1500 rpm for 24 hours. After the reaction, we washed the mixture with 40 mL of diethyl ether and then with a solution containing 3 mL of MeOH and 40 mL of diethyl ether three times. We used the same washing procedure as we previously described. Then we dried the pellet overnight in a vacuum dessicator and resuspended the dried PS-PEO-N<sub>3</sub> pellet in deionized (DI) water to a concentration of 100 mM.

We attached the azide-modified PS-PEO copolymer to the surface of polystyrene colloids using a physical grafting method. We first adsorbed PS-PEO-N<sub>3</sub> to the surface of polystyrene colloids by mixing 160  $\mu$ L of 100 mM PS-PEO-N<sub>3</sub>, 160  $\mu$ L of tetrahydrofuran, 40  $\mu$ L of deionized (DI) water, and 40  $\mu$ L of 10% (v/v) 600 nm-diameter PS particles (Molecular Probes), and then vortexed the mixture for 30 minutes. Next, we diluted the mixture 10× with DI water, washed the particles with DI water five times, and concentrated the particles back to 1% (v/v) after washing.

We dyed particles with different fluorophores so that we could distinguish between different particle species. Specifically, we labeled three types of particles, one with nile red, one with pyromethene green, and one with both. We first made saturated solutions of fluorescent dye dissolved in toluene. We mixed 4  $\mu$ L of 10% saturated nile red or 50% saturated pyromethene green in toluene and 400  $\mu$ L 1% azide-functionalized PS particles and rotated end-over-end for 7 hours. Next we opened the sample to air and heated it in an oven at 90 °C for 12 minutes. After that, we washed the dyed particles five times in DI water by centrifugation and resuspension.

Finally, we attached DNA molecules to the azide-modified PS-PEO copolymers using strain-promoted click chemistry.



We mixed 40  $\mu\text{L}$  of 1% azide-functioned PS particles, 10  $\mu\text{L}$  of 100  $\mu\text{M}$  ssDNA, and 150  $\mu\text{L}$  1 $\times$  TE/1 M NaCl buffer containing 0.05 wt% Pluronic F127 (Merck), and heated the sample in an oven at 70  $^{\circ}\text{C}$  for 24 hours. After the reaction, we washed the DNA-coated particles with DI water five times by centrifugation and resuspension.

#### 4.2 PER reaction

To append new sequences onto the DNA grafted to the particles (scale: 50  $\mu\text{L}$  of a 0.1 wt% particle suspension), we used an adapted version of the primer exchange reaction (PER) described in ref. 30: first we prepared a PER reaction mixture containing final concentrations of 1 $\times$  Thermopol DNA polymerase buffer (New England Biolabs, provided at 10 $\times$  concentration with the DNA polymerase), 12.5 mM MgCl<sub>2</sub> (New England Biolabs, provided as a 100  $\mu\text{L}$  solution with the DNA polymerase), and 100 mM of each dATP (deoxyribose adenine triphosphate, ThermoFisher, 10 mM), dCTP, and dTTP. No dGTP was added to the mixture because only ACT sequences were appended onto particles and a G-C pair was used as a stop sequence (see ESI<sup>†</sup> Section: “Design considerations”). Note, for the purple co-assembler particles in Fig. 4 a different reaction mixture was prepared containing dGTP, but no dCTP. There an AGT sequence was appended onto the particle and a C-G pair was used as stop sequence. All solutions were prepared in Millipore purified water. DNA was stored at -20  $^{\circ}\text{C}$  and DNA-coated particles were stored at 4  $^{\circ}\text{C}$ .

For the primer exchange reaction, we mixed 5  $\mu\text{L}$  of 1 wt% DNA-coated particle suspension to a final concentration of 0.1 wt%; 5  $\mu\text{L}$  of 1  $\mu\text{M}$  DNA hairpin solution to a final concentration of 100 nM; 25  $\mu\text{L}$  of the premixed PER reaction mixture; and 1  $\mu\text{L}$  of 8 U  $\mu\text{L}^{-1}$  Bst Large Fragment DNA polymerase (New England Biolabs) to a final concentration of 0.13 U  $\mu\text{L}^{-1}$ ; and 14  $\mu\text{L}$  water to a total reaction volume of 50  $\mu\text{L}$  in a 1 mL Eppendorf tube. For Fig. S1 (ESI<sup>†</sup>) larger concentrations of Bst DNA polymerase were used as indicated in the figures. For Fig. 2 and Fig. S2 (ESI<sup>†</sup>) varying hairpin concentrations were used as indicated in the figures.

The reaction mixture was rotated at room temperature (approximately 24  $^{\circ}\text{C}$ ) for 1 hour, after which the reaction was terminated by washing. We found that the rotation to prevent sedimentation is not essential for reaction times under 2 hours. The sample should appear homogeneously milky throughout the reaction. We washed by centrifuging the particles 4 times at 3000  $\times g$  for 3 minutes, removing 45  $\mu\text{L}$  reaction mixture each time and resuspending the particles in 50  $\mu\text{L}$  by adding 45  $\mu\text{L}$  of water. After centrifugation the sample should become entirely transparent with a small white pellet at the bottom of the Eppendorf tube. Reaction times were varied for Fig. 2 and 3c as indicated in the figures.

Except for the DBCO-modified DNA, all DNA was purchased unpurified (*i.e.* standard desalting) from Integrated DNA Technologies, in the “lab ready” formulation (dissolved in IDTE buffer at 100  $\mu\text{M}$ ). The DBCO-modified DNA (Integrated DNA Technologies) was HPLC purified.

#### 4.3 Crystallization experiments

To prepare samples for crystallization we mixed 1  $\mu\text{L}$  of 1% (v/v) each of two complementary DNA-coated particle types (2  $\mu\text{L}$  total) with  $\mu\text{L}$  of 1 $\times$  TE Buffer with 500 mM NaCl, for a total sample volume of 4  $\mu\text{L}$ . We take 1.6  $\mu\text{L}$  of the solution and pipette it onto a plasma-cleaned 24 mm  $\times$  60 mm coverslip in the center of a thin, open ring of high vacuum grease (Dow Corning). A second piece of 15 mm  $\times$  15 mm plasma-cleaned coverslip is placed on top, making a seal with the vacuum grease. When sealing the chamber we removed as much air as possible without allowing the solution to move past the vacuum grease ring before it closes off. For longer timescale experiments, an additional seal of UV glue was used on the edges of the coverslip to prevent shear on the chamber as well as reduce further the chance for evaporation to break the grease seal.

To control the temperature of the sample, we taped it to home-built temperature stage consisting of a peltier element with a thermistor controlled by a PID controller. We started experiments by raising the temperature to the point where all aggregates melted. The sample was left at this temperature for approximately 30 minutes until the particle density became uniform across the chamber. The temperature was then lowered in 0.5  $^{\circ}\text{C}$  steps and held for 5 minutes at each point. By looking at the fraction of particles that have aggregated at each temperature we found the melting temperature, where 50% of particles are aggregated. To form crystals, we melted the sample and then held the temperature  $\sim$ 0.3  $^{\circ}\text{C}$  above the melting temperature. It took about three hours for crystal domains to form.

We imaged the samples using either an inverted, brightfield microscope (Nikon Eclipse TE2000-E) or a confocal microscope (Leica SP8) equipped with 20 $\times$  air, 40 $\times$  air, and a 60 $\times$  oil immersion objectives.

In the melting temperature measurements, we quantified the fraction of single particles using particle-tracking software.<sup>51</sup> The software cannot distinguish all particles in the clusters, but this undercount does not affect our results; we can nonetheless accurately measure the melting temperature, which is the point at which the number of single particles changes most steeply.

#### 4.4 Flow cytometry

Flow cytometry experiments were performed on a BD FACS-Canto high-throughput analytical flow cytometer. Samples were prepared in a 1 mL Eppendorf tube by diluting 1  $\mu\text{L}$  of 0.1 wt% into 100  $\mu\text{L}$  buffer containing 10 mM Tris-HCl (pH = 7.5), 1 M NaCl, and 1 mM EDTA and varying concentrations of fluorescently labeled DNA complementary to the DNA on the particle. In Fig. 2 we added 10  $\mu\text{L}$  of  $\mu\text{M}$  reporter strand to a final concentration of 100 nM. In Fig. S4 (ESI<sup>†</sup>), the concentrations varied as indicated in the figure.

The samples were left to equilibrate for at least one hour, then they were diluted in 400  $\mu\text{L}$  of the same buffer (without additional reporter strand), vortexed, and transferred to a flow cytometry tube immediately. The fluorescent signal of

10 thousand particles was collected over approximately 5 minutes, using the low flow rate setting.

Of all measured events, only the subpopulation involving single particles was selected by applying a gate based on forward and side scatter intensity. Events involving dimers, or larger aggregates were discarded. Data were analyzed in FCS Express 6 Flow Research Edition.

#### 4.5 Gel electrophoresis

We measured whether PER on particles led to any unintended side products, such as shorter or longer strands than the intended product. To visualize the length of a DNA strand in an electrophoresis gel, it needs to be removed from the particle. Therefore, we PER-edited particles coated with DNA *via* the streptavidin–biotin bond. This bond can be broken by heat denaturing in formamide, to release the DNA after the reaction.

We first prepared DNA-coated particles from streptavidin-coated particles (1  $\mu$ m in diameter, Bangs Labs) by mixing 0.1 wt% particles with  $\mu$ M biotin-functionalized DNA in a total volume of 50  $\mu$ L. The particles were placed on a rotator for 1 hour and washed by centrifugation and resuspension (3 $\times$ , 3 min at 3000 rcf). Then the DNA on their surface was updated using PER according to the description above. The reaction was stopped and the DNA removed from the particle simultaneously by adding loading buffer in formamide and heat denaturing the sample at 95 °C for 5 minutes. This step deactivated the DNA polymerase and broke the biotin–streptavidin bond. The samples were then centrifuged and the supernatants were loaded into a 15% polyacrylamide gel in a bath of 1 $\times$  Tris/Borate/EDTA (TBE) buffer heated to 65 °C. Then 100 V was applied for 2 hours. The gels were stained with Sybr gold dye and imaged using a SynGene Genebox gel imager operated with the Genesys software.

#### Author contributions

P. G. M., R. S., & W. B. R. conceived the experiments. P. G. M., T. E. V., & H. F. performed the experiments and analysis. All authors contributed to writing of the paper.

#### Conflicts of interest

There are no conflicts to declare.

#### Acknowledgements

We thank Hanhvy Bui for her help with flow cytometry. P. G. M. and R. S. acknowledge funding from the ARO (grant number W911NF2010057) and the DOE (grant number DE-SC0010426) for efforts involving flow cytometry. P. G. M. acknowledges funding by the American Institute of Physics through the Robert H.G. Helleman Memorial Fellowship. H. F., T. E. V., and W. B. R. acknowledge NSF funding (grant number DMR-1710112, DMR-2214590) and funding from the Brandeis Bio-inspired Soft Materials MRSEC (grant number DMR-2011846).

W.B.R acknowledges support from the Smith Family Foundation.

## References

- 1 W. B. Rogers, W. M. Shih and V. N. Manoharan, Using DNA to Program the Self-Assembly of Colloidal Nanoparticles and microparticles, *Nat. Rev. Mat.*, 2015, **1**, 1–14, DOI: [10.1038/natrevmat.2016.8](https://doi.org/10.1038/natrevmat.2016.8).
- 2 C. A. Mirkin, R. L. Letsinger, R. C. Mucic and J. J. Storhoff, A DNA-based Method For Rationally Assembling Nanoparticles into Macroscopic Materials, *Nature*, 1996, **382**, 607–609, DOI: [10.1038/382607a0](https://doi.org/10.1038/382607a0).
- 3 A. P. Alivisatos, K. P. Johnson, X. Peng, T. E. Wilson, C. J. Loweth, M. P. Bruchez Jr. and P. G. Schultz, Organization of Nanocrystal Molecules Using DNA, *Nature*, 1996, **382**, 609–611, DOI: [10.1038/382609a0](https://doi.org/10.1038/382609a0).
- 4 W. B. Rogers and J. C. Crocker, Direct Measurements of DNA-Mediated Colloidal Interactions and Their Quantitative Modeling, *Proc. Natl. Acad. Sci. U. S. A.*, 2011, **108**, 15687–15692, DOI: [10.1073/pnas.1109853108](https://doi.org/10.1073/pnas.1109853108).
- 5 W. Liu, J. Halverson, Y. Tian, V. T. Tkachenko and O. Gang, Self-Organized Architectures from Assorted DNA-Framed Nanoparticles, *Nat. Chem.*, 2016, **8**, 867–873, DOI: [10.1038/nchem.2540](https://doi.org/10.1038/nchem.2540).
- 6 S. Y. Park, A. K. R. Lytton-Jean, B. Lee, S. Weigand, G. C. Schatz and C. A. Mirkin, DNA-Programmable Nanoparticle Crystallization, *Nature*, 2008, **451**, 553–556, DOI: [10.1038/nature06508](https://doi.org/10.1038/nature06508).
- 7 E. Auyeung, T. I. N. G. Lee, A. J. Senesi, A. L. Schmucker, B. C. Pals, M. Olvera de la Cruz and C. A. Mirkin, DNA-Mediated Nanoparticle Crystallization into Wulff Polyhedra, *Nature*, 2014, **505**, 73–77, DOI: [10.1038/nature12739](https://doi.org/10.1038/nature12739).
- 8 W. B. Rogers and V. N. Manoharan, Programming Colloidal Phase Transitions With DNA Strand Displacement, *Science*, 2015, **347**, 639–642, DOI: [10.1126/science.1259762](https://doi.org/10.1126/science.1259762).
- 9 Y. Wang, I. C. Jenkins, J. T. McGinley, T. Sinno and J. C. Crocker, Colloidal Crystals with Diamond Symmetry at Optical Lengthscales, *Nat. Commun.*, 2017, **8**, 14173, DOI: [10.1038/ncomms14173](https://doi.org/10.1038/ncomms14173).
- 10 A. McMullen, M. Holmes-Cerfon, F. Sciortino, A. Y. Grosberg and J. Brujic, Freely Jointed Polymers Made of Droplets, *Phys. Rev. Lett.*, 2018, **121**, 138002, DOI: [10.1103/PhysRevLett.121.138002](https://doi.org/10.1103/PhysRevLett.121.138002).
- 11 R. Verweij, P. G. Moerman, N. E. G. Ligthart, L. P. P. Huijnen, J. Groenewold, W. K. Kegel, A. Van Blaaderen and D. J. Kraft, Flexibility-Induced Effects in the Brownian Motion of Colloidal Trimers, *Phys. Rev. Res.*, 2020, **2**, 033136, DOI: [10.1103/PhysRevResearch.2.033136](https://doi.org/10.1103/PhysRevResearch.2.033136).
- 12 M. Y. Ben Zion, X. He, C. C. Maass, R. Sha, N. C. Seeman and P. M. Chaikin, Self-Assembled Three-Dimensional Chiral Colloidal Architecture, *Science*, 2017, **358**, 633–636, DOI: [10.1126/science.aan5404](https://doi.org/10.1126/science.aan5404).
- 13 M. Todhunter, N. Jee, A. Hughes, M. C. Coyle, A. Cerchiari, J. Farlow, J. C. Garbe, M. A. LaBarge, T. A. Desai and



Z. J. Gartner, Programmed Synthesis of Three-Dimensional Tissues, *Nat. Methods*, 2015, **12**, 975–981, DOI: [10.1038/nmeth.3553](https://doi.org/10.1038/nmeth.3553).

14 R. K. Cersonsky, J. Antonaglia, B. D. Dice and S. C. Glotzer, The Diversity of Three-Dimensional Photonic Crystals, *Nat. Commun.*, 2021, **12**, 2543, DOI: [10.1038/s41467-021-22809-6](https://doi.org/10.1038/s41467-021-22809-6).

15 M. He, J. P. Gales, É. Ducrot, Z. Gong, G.-R. Yi, S. Sacanna and D. J. Pine, Colloidal Diamond, *Nature*, 2020, **585**, 524–529, DOI: [10.1038/s41586-020-2718-6](https://doi.org/10.1038/s41586-020-2718-6).

16 E. Ducrot, M. He, G. R. Yi and D. J. Pine, Colloidal Alloys with Preassembled Clusters and Spheres, *Nat. Mater.*, 2017, **16**, 652–657, DOI: [10.1038/nmat4869](https://doi.org/10.1038/nmat4869).

17 A. Hensley, W. M. Jacobs and W. B. Rogers, Self-Assembly of Photonic Crystals by Controlling the Nucleation and Growth of DNA-Coated Colloids, *Proc. Natl. Acad. Sci. U. S. A.*, 2022, **119**, e2114050118, DOI: [10.1073/pnas.2114050118](https://doi.org/10.1073/pnas.2114050118).

18 J. S. Oh, S. Lee, S. C. Glotzer, G.-R. Yi and D. J. Pine, Colloidal Fibers and Rings by Cooperative Assembly, *Nat. Commun.*, 2019, **10**(1), 3936, DOI: [10.1038/s41467-019-11915-1](https://doi.org/10.1038/s41467-019-11915-1).

19 Z. Zeravcic and M. P. Brenner, Self-Replicating Colloidal Clusters, *Proc. Natl. Acad. Sci. U. S. A.*, 2014, **111**, 1748–1753, DOI: [10.1073/pnas.1313601111](https://doi.org/10.1073/pnas.1313601111).

20 H. Dehne, A. Reitenbach and A. R. Bausch, Transient Self-Organisation of DNA Coated Colloids Directed by Enzymatic Reactions, *Sci. Rep.*, 2019, **9**, 7350, DOI: [10.1038/s41598-019-43720-7](https://doi.org/10.1038/s41598-019-43720-7).

21 J. Moon, I. S. Jo, E. Ducrot, J. S. Oh, D. J. Pine and G.-R. Yi, DNA-Coated Microspheres and Their Colloidal Superstructures, *Macromol. Res.*, 2018, **26**, 1085–1094, DOI: [10.1007/s13233-018-6151-8](https://doi.org/10.1007/s13233-018-6151-8).

22 A. J. Kim, P. L. Biancaniello and J. C. Crocker, Engineering DNA-Mediated Colloidal Crystallization, *Langmuir*, 2006, **22**, 1991–2001, DOI: [10.1021/la0528955](https://doi.org/10.1021/la0528955).

23 L. Di Michele, F. Varrato, J. Kotar, S. H. Nathan, G. Foffi and E. Eiser, Multistep Kinetic Self-Assembly of DNA-Coated Colloids, *Nat. Commun.*, 2013, **4**, 2007, DOI: [10.1038/ncomms3007](https://doi.org/10.1038/ncomms3007).

24 Y. Wang, Y. Wang, X. Zheng, E. Ducrot, M. G. Lee, G.-R. Yi, M. Weck and D. J. Pine, Synthetic Strategies Toward DNA-Coated Colloids That Crystallize, *J. Am. Chem. Soc.*, 2015, **137**(33), 10760–10766.

25 J. S. Oh, Y. Wang, D. J. Pine and G.-R. Yi, High-Density PEO-*b*-DNA Brushes on Polymer Particles for Colloidal Superstructures, *Chem. Mater.*, 2015, **27**, 8337–8344, DOI: [10.1021/acs.chemmater.5b03683](https://doi.org/10.1021/acs.chemmater.5b03683).

26 J. S. Oh, M. He, G.-R. Yi and D. J. Pine, High-Density DNA Coatings on Carboxylated Colloids by DMTMM- and Azide-Mediated Coupling Reactions, *Langmuir*, 2020, **36**(13), 3583–3589, DOI: [10.1021/acs.langmuir.9b03386](https://doi.org/10.1021/acs.langmuir.9b03386).

27 Y. Wang, Y. Wang, X. Zheng, E. Ducrot, J. S. Yodh, M. Weck and D. J. Pine, Crystallization of DNA-Coated Colloids, *Nat. Commun.*, 2015, **6**, 7253, DOI: [10.1038/ncomms8253](https://doi.org/10.1038/ncomms8253).

28 H. Fang, M. F. Hagan and W. B. Rogers, Two-Step Crystallization and Solid–Solid Transitions in Binary Colloidal Mixtures, *Proc. Natl. Acad. Sci. U. S. A.*, 2020, **117**, 27927–27933, DOI: [10.1073/pnas.2008561117](https://doi.org/10.1073/pnas.2008561117).

29 Integrated DNA Technologies (IDT) provides tailored DNA sequences with DBCO modifications on the 3' or 5' end: <https://www.idtdna.com/pages/education/decoded/article/need-a-non-standard-modification>.

30 J. Y. Kishi, T. E. Schaus, N. Gopalkrishnan, F. Xuan and P. Yin, Programmable Autonomous Synthesis of Single-Stranded DNA, *Nat. Chem.*, 2018, **10**, 155–164, DOI: [10.1038/nchem.2872](https://doi.org/10.1038/nchem.2872).

31 P. G. Moerman, M. Gavrilov, T. J. Ha and R. Schulman, Catalytic DNA Polymerization Can Be Expedited by Active Product Release, *Angew. Chem., Int. Ed.*, 2022, **61**(24), e202114581.

32 X. Tong and L. M. Smith, Solid-Phase Method for the Purification of DNA Sequencing Reactions, *Anal. Chem.*, 1992, **64**, 2672–2677, DOI: [10.1021/ac00046a004](https://doi.org/10.1021/ac00046a004).

33 F. Cui, S. Marbach, J. A. Zheng, M. Holmes-Cerfon and D. J. Pine, Comprehensive View of Microscopic Interactions Between DNA-Coated Colloids, *Nat. Commun.*, 2022, **13**, 2304, DOI: [10.1038/s41467-022-29853-w](https://doi.org/10.1038/s41467-022-29853-w).

34 R. Dreyfus, M. E. Leunissen, R. Sha, R. V. Tkachenko, N. C. Seeman, D. J. Pine and P. M. Chaikin, Simple Quantitative Model for the Reversible Association of DNA Coated Colloids, *Phys. Rev. Lett.*, 2009, **102**, 048301, DOI: [10.1103/PhysRevLett.102.048301](https://doi.org/10.1103/PhysRevLett.102.048301).

35 N. Geerts and E. Eiser, DNA-Functionalized Colloids: Physical Properties and Applications, *Soft Matter*, 2010, **6**, 4647–4660, DOI: [10.1039/C001603A](https://doi.org/10.1039/C001603A).

36 J. C. Rolando, E. Jue, J. T. Barlow and R. F. Ismagilov, Real-Time Kinetics and High-Resolution Melt Curves in Single-Molecule Digital LAMP to Differentiate and Study Specific and Non-Specific Amplification, *Nucleic Acids Res.*, 2020, **48**, e42, DOI: [10.1093/nar/gkaa099](https://doi.org/10.1093/nar/gkaa099).

37 N. V. Zyrina, V. N. Antipova and L. A. Zheleznyaya, Ab Initio Synthesis by DNA Polymerases, *FEMS Microbiol. Lett.*, 2014, **351**, 1–6, DOI: [10.1111/1574-6968.12326](https://doi.org/10.1111/1574-6968.12326).

38 P. K. Jana and B. M. Mognetti, Self-Assembly of Finite-Sized Colloidal Aggregates, *Soft Matter*, 2020, **16**, 5915–5924, DOI: [10.1039/DOSM00234H](https://doi.org/10.1039/DOSM00234H).

39 M. Parvez and M. B. Zanjani, Synthetic Self-Limiting Structures Engineered with Defective Colloidal Clusters, *Adv. Funct. Mater.*, 2020, **30**, 2003317, DOI: [10.1002/adfm.202003317](https://doi.org/10.1002/adfm.202003317).

40 A. Murugan, Z. Zeravcic, M. P. Brenner and S. Leibler, Multifarious Assembly Mixtures: Systems Allowing Retrieval of Diverse Stored Structures, *Proc. Natl. Acad. Sci. U. S. A.*, 2015, **112**, 54–59, DOI: [10.1073/pnas.1413941112](https://doi.org/10.1073/pnas.1413941112).

41 K. Wu, L. Feng, R. Sha and P. Chaikin, Polygamous Particles, *Proc. Natl. Acad. Sci. U. S. A.*, 2012, **109**, 18731–18736, DOI: [10.1073/pnas.1207356109](https://doi.org/10.1073/pnas.1207356109).

42 J. H. Cho, R. Cerbino and I. Bischofberger, Emergence of Multiscale Dynamics in Colloidal Gels, *Phys. Rev. Lett.*, 2020, **124**, 08800, DOI: [10.1103/PhysRevLett.124.088005](https://doi.org/10.1103/PhysRevLett.124.088005).

43 Z. M. Sherman, A. M. Green, M. P. Howard, E. V. Anslyn, T. M. Truskett and D. J. Milliron, Colloidal Nanocrystal Gels from Thermodynamic Principles, *Acc. Chem. Res.*, 2021, **54**, 798–807, DOI: [10.1021/acs.accounts.0c00796](https://doi.org/10.1021/acs.accounts.0c00796).



44 M. Nabizadeh and S. Jamali, Life and Death of Colloidal Bonds Control the Rate-Dependent Rheology of Gels, *Nat. Commun.*, 2021, **12**, 4274, DOI: [10.1038/s41467-021-24416-x](https://doi.org/10.1038/s41467-021-24416-x).

45 J. Z. Hui, S. Tamsen, Y. Song and A. Tsourkas, LASIC: Light Activated Site-Specific Conjugation of Native IgGs, *Bioconjug. Chem.*, 2015, **19**, 1456, DOI: [10.1021/acs.bioconjchem.5b00275](https://doi.org/10.1021/acs.bioconjchem.5b00275).

46 D. Gresham, M. J. Dunham and D. Bodstein, Comparing Whole Genomes Using DNA Microarrays, *Nat. Rev. Genet.*, 2008, **9**, 291–302, DOI: [10.1038/nrg2335](https://doi.org/10.1038/nrg2335).

47 J. Lowensohn, B. Oyarzún, G. N. Paliza, B. M. Mognetti and W. B. Rogers, Linker-Mediated Phase Behavior of DNA-Coated Colloids, *Phys. Rev. X*, 2019, **9**, 041054, DOI: [10.1103/PhysRevX.9.041054](https://doi.org/10.1103/PhysRevX.9.041054).

48 J. Lowensohn, A. Hensley, N. Perlow-Zelman and W. B. Rogers, Linker-Self-Assembly and Crystallization of DNA-Coated Colloids via Linker-Encoded Interactions, *Langmuir*, 2020, **36**, 7100–7108, DOI: [10.1021/acs.langmuir.9b03391](https://doi.org/10.1021/acs.langmuir.9b03391).

49 S. De and R. Klajn, Dissipative Self-Assembly Driven by the Consumption of Chemical Fuels, *Adv. Mater.*, 2018, **30**, 1706750, DOI: [10.1002/adma.201706750](https://doi.org/10.1002/adma.201706750).

50 B. G. P. Van Ravenstein, I. K. Voets, W. K. Kegel and R. Elkema, Out-of-Equilibrium Colloidal Assembly Driven by Chemical Reaction Networks, *Langmuir*, 2020, **36**, 10639–10656, DOI: [10.1021/acs.langmuir.0c01763](https://doi.org/10.1021/acs.langmuir.0c01763).

51 J. Crocker and D. Grier, Methods of Digital Video Microscopy for Colloidal Studies, *J. Colloid Interface Sci.*, 1996, **179**, 298–310, DOI: [10.1006/jcis.1996.0217](https://doi.org/10.1006/jcis.1996.0217).

52 E. W. Gehrels, W. B. Rogers, Z. Zeravcic and V. N. Manoharan, Programming Directed Motion with DNA-Grafted Particles, *ACS Nano*, 2022, **16**, 9195–9202, DOI: [10.1021/acs.nano.2c01454](https://doi.org/10.1021/acs.nano.2c01454).

